ResearchGate

See discussions, stats, and author profiles for this publication at: https://www.researchgate.net/publication/42805426

Effect of Annealing on the Properties of Indium–Tin–Oxynitride Films as Ohmic Contacts for GaN–Based Optoelectronic Devices

ARTICLE *in* ACS APPLIED MATERIALS & INTERFACES · JULY 2009

Impact Factor: 6.72 · DOI: 10.1021/am900138f · Source: PubMed

CITATIONS
6

READS
36

11 AUTHORS, INCLUDING:

Gernot Ecke
Technische Universität Ilmenau
97 PUBLICATIONS **898** CITATIONS
SEE PROFILE

J.A. Schaefer
Technische Universität Ilmenau
202 PUBLICATIONS **3,844** CITATIONS
SEE PROFILE

Stefan Krischok
Technische Universität Ilmenau
136 PUBLICATIONS **1,636** CITATIONS
SEE PROFILE

E. Aperathitis
Foundation for Research and Technology - …
68 PUBLICATIONS **482** CITATIONS
SEE PROFILE

Available from: E. Aperathitis
Retrieved on: 31 January 2016

Effect of Annealing on the Properties of Indium−Tin−Oxynitride Films as Ohmic Contacts for GaN-Based Optoelectronic Devices

Marcel Himmerlich,[†,‡] Maria Koufaki,[§,⊥] Gernot Ecke,[†] Christof Mauder,[†] Volker Cimalla,[†,∥] Juergen A. Schaefer,[†] Antonis Kondilis,[⊥] Nikos T. Pelekanos,[⊥,#] Mircea Modreanu,[▽] Stefan Krischok,[*,†] and Elias Aperathitis[⊥]

Institute of Micro- and Nanotechnologies, TU Ilmenau, P.O. Box 100565, 98684 Ilmenau, Germany, Physics Department, University of Crete, P.O. Box 2208, 71003 Heraklion, Crete, Greece, Microelectronics Research Group, Institute of Electronic Structure & Laser, Foundation for Research and Technology - Hellas, P.O. Box 1385, 71110 Heraklion, Crete, Greece, Materials Science & Technology Department, University of Crete, P.O. Box 2208, 71003 Heraklion, Crete, Greece, and Photonics Group, Tyndall National Institute, Lee Maltings, Prospect Row, Cork, Ireland

Downloaded by TECHNISCHE UNIV ILMENAU on July 29, 2009
Published on June 9, 2009 on http://pubs.acs.org | doi: 10.1021/am900138f

ABSTRACT Indium−tin−oxynitride (ITON) films have been fabricated by rf sputtering from an indium−tin−oxide target in nitrogen plasma. The influence of postdeposition annealing up to 800 °C is analyzed by electrical, optical, and surface characterization of the films in comparison to indium−tin−oxide (ITO) films fabricated in argon plasma. High-temperature annealing resulted in ITO(N) films with similar carrier concentrations. However, the resistivity and optical transmittance of the ITON films were higher than those of the ITO films. Photoelectron spectroscopy revealed that nitrogen is incorporated into the ITON structure in an unbound state as well as through the formation of metal−nitrogen and oxynitride bonds that decorate oxygen vacancies. When the core level electron spectra of ITO and ITON films are compared, a correlation between carrier concentration and the incorporated nitrogen is found. Changes in ITON electrical properties are mainly induced by the release of nitrogen at temperatures above 550 °C. In this context, ohmic contact behavior was achieved for ITON on p-type GaN after annealing at 600 °C, while no ohmic contact could be realized using ITO.

KEYWORDS: oxides • oxynitrides • semiconductors • sputtering • photoelectron spectroscopy

INTRODUCTION

Indium−tin−oxide (ITO) is, in addition to ZnO, SnO_2, and CdO, a very commonly used transparent conductive oxide. When ITO is utilized for optoelectronic devices, it serves as optical as well as contact material. Even though ITO is a wide band gap material (the onset of optical absorption varies between 3.5 and 4.0 eV, depending on the deposition technique), it is an n-type degenerate semiconductor with oxygen vacancies and tin atoms at indium sites mainly determining the conductivity of the material. Due to the lack of p-type oxides with similar properties (wide band gap and at the same time high conductivity) ITO has been used in many III−V-based optoelectronic devices. In particular, for the case of devices based on the wide band gap III−nitride compounds, ITO has been used as the ohmic contact on p-GaN layers (1, 2).

It should be noted that the metallic ohmic contact formation on p-GaN is still a developing technology, mainly due to the low doping density of p-GaN. Attempts to improve or modify the properties of ITO for other technological applications have been reported, such as changing its composition using H_2^+ and O^+ implantation (3) or adding Zn (4), Ag (5), or Zr (6) during deposition.

In a previous study we have shown that the introduction of nitrogen in the plasma chamber during rf sputter deposition of ITO results in the incorporation of nitrogen into the film structure and the formation of ITON films (7). Deposition performed in pure nitrogen plasma, followed by postdeposition annealing at 400 °C, resulted in ITON films with improved optical properties but inferior electrical properties compared to conventional ITO films deposited in argon plasma (8).

In this work, we investigate the chemical structure of the incorporated nitrogen in ITON as well as the surface composition of ITO(N), by employing photoelectron spectrosco-

* To whom correspondence should be addressed. E-mail: stefan.krischok@tu-ilmenau.de.
Received for review March 3, 2009 and accepted May 24, 2009
† TU Ilmenau.
‡ Current address: Fraunhofer Institute for Manufacturing Technology and Applied Materials Research, Wiener Str. 12, 28359 Bremen, Germany.
§ Physics Department, University of Crete.
∥ Current address: Fraunhofer Institute for Applied Solid State Physics, Tullastr. 72, 79108 Freiburg, Germany.
⊥ Foundation for Research and Technology - Hellas.
Materials Science & Technology Department, University of Crete.
▽ Tyndall National Institute.
DOI: 10.1021/am900138f
© 2009 American Chemical Society

Downloaded by TECHNISCHE UNIV ILMENAU on July 29, 2009
Published on June 9, 2009 on http://pubs.acs.org | doi: 10.1021/am900138f

py, just after deposition and after annealing at temperatures above 400 °C. A comparison of the results derived from surface characterization is made to the results from the analysis of electrical and optical properties. Furthermore, the potential of ohmic contact formation on p-type GaN layers is evaluated.

EXPERIMENTAL SECTION

The ITON and ITO thin films were deposited by rf sputtering from an indium−tin−oxide (80% In_2O_3−20% SnO_2) target in pure N_2 or Ar plasma, respectively. Details of the sputtering procedure have been reported elsewhere (9). All films were prepared at 5 mTorr pressure and different rf powers, varying between 150 and 550 W. Depending on the requirements of the experimental techniques used in this study, the deposition was performed on different substrates: double side polished sapphire for the electrical and optical characterization of the films, p-type (100) Si wafers (1−10 Ωcm) for electron spectroscopy studies, and commercially available p-type GaN templates (TDI Inc.), having a hole concentration of $\sim 4 \times 10^{17}$ cm^{-3}, to study the contact properties between substrate and deposited film. Material properties were investigated just after rf sputter deposition and after postdeposition annealing performed in a rapid thermal annealing (RTA) system (Jipelec FAV4) for 1 min under a nitrogen atmosphere (flow 450 sccm) at temperatures up to 800 °C.

The thickness of the films was 150−200 nm, as measured by a profilometer, and the surface morphology was examined by atomic force microscopy (AFM). The optical properties of the films were recorded in the UV−near-IR region (Varian, Cary 50), and the electrical properties were determined by Hall measurements using the four-probe Van der Pauw technique.

The surface chemical composition, including the presence and the role of nitrogen in the ITON films, was examined in a UHV system by X-ray photoelectron spectroscopy (XPS) using monochromated Al Kα radiation ($h\nu$ = 1486.7 eV) and a hemispherical electron analyzer, resulting in an overall energy resolution of <0.6 eV of the $Ag3d_{5/2}$ level for the chosen experimental conditions (10, 11). XPS measurements were performed after gentle Ar^+ ion bombardment of the sample surface, in order to remove any adsorbed contaminants which could originate from transferring the sample through ambient conditions. Special care has been taken to avoid metal formation at the surface due to preferential sputtering. Additionally, quadrupole mass spectroscopy (QMS) was used in order to analyze species desorbing from ITON during annealing under UHV conditions. Furthermore, Auger-electron spectroscopy (AES) depth profiling measurements were performed using a Thermo Microlab 350 instrument equipped with a high spatial resolution field emission electron beam column and a high energy resolution hemispherical analyzer.

For the characterization of contact properties on p-GaN, the circular transmission line method (c-TLM) was employed and the patterns were formed using standard photolithographic techniques. For this purpose, the p-GaN surface was treated by aqua regia prior to insertion into the sputtering chamber and an in situ plasma etching process in N_2 prior to ITON or ITO deposition.

RESULTS AND DISCUSSION

Electrical and Optical Properties. In order to examine the effect of annealing on the film properties and to correlate their properties with the incorporated nitrogen, the ITON and ITO films were annealed at temperatures above 400 °C. The resistivity and carrier concentration of the ITO and ITON films change strongly as a function of annealing temperature, in particular above 400 °C. Therefore, special attention has been drawn to the XPS characterization of as-prepared films and samples annealed at 400 and 600 °C, respectively. The results for the particular samples investigated by XPS are plotted in Figure 1. Nevertheless, the same observation has been made for various sets of samples. Upon annealing, both sample types became more conductive, with the ITON remaining a higher resistivity and lower electron concentration compared to the ITO films. However, the carrier concentrations of both types became almost the same as the annealing temperature increased to 600 °C. For annealing above 600 °C only very small additional changes in resistivity and carrier concentration have been observed. The mobility determined by Hall measurements of the ITON films was between 2 and 5 $cm^2/(V\ s)$, regardless of the annealing temperature, whereas the mobility of the ITO films increased up to 26 $cm^2/(V\ s)$ with annealing temperature.

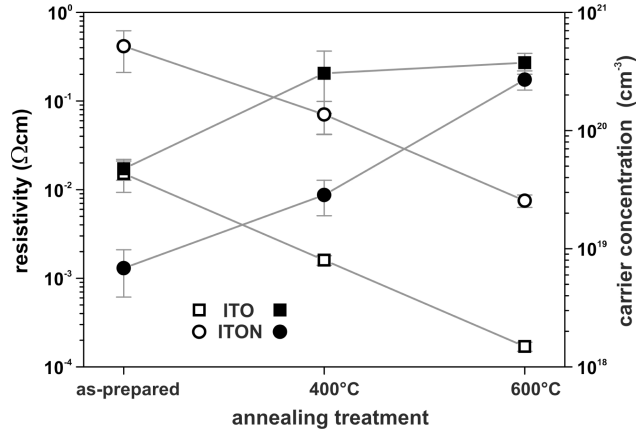

FIGURE 1. Electrical properties (resistivity, open symbols; carrier concentration, solid symbols) of ITO (squares) and ITON (circles) as a function of annealing temperature.

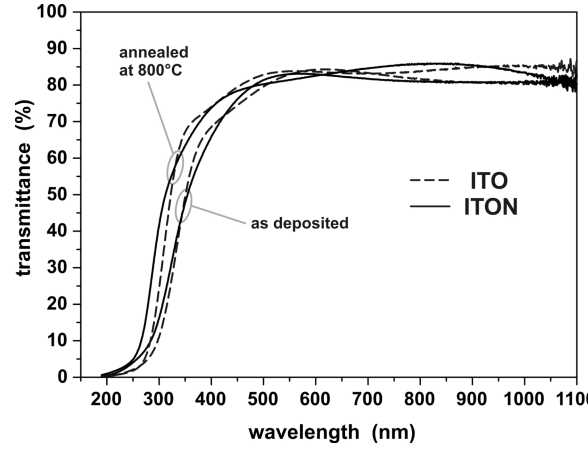

FIGURE 2. Transmittance of ITO and ITON thin films measured after deposition and after RTA at 800 °C.

The optical properties of the films were monitored as a function of annealing temperature. The measured transmittance of ITO and ITON films directly after deposition and after successive annealing up to 800 °C is shown in Figure 2. The high annealing temperature has led to improved transmission curves, with a transmittance higher than 40% at a wavelength of 300 nm for ITON films and 320 nm for

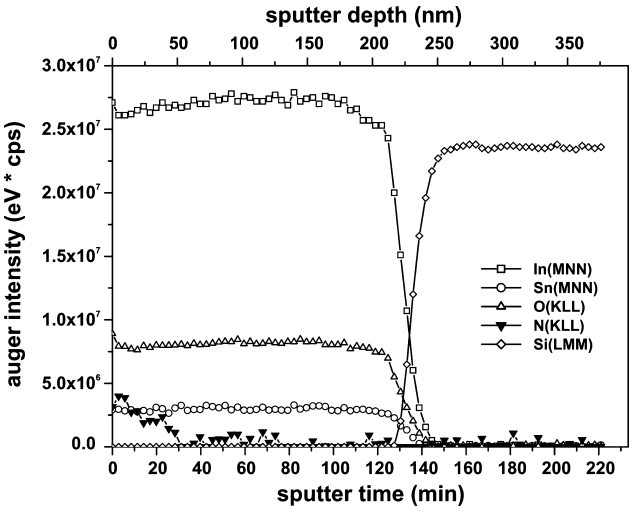

FIGURE 3. Auger electron spectroscopy depth profile of the In, Sn, O, Si, and N distribution in an as-prepared 230 nm thick ITON film. Note that the sputter depth has been estimated from the optically determined film thickness of the ITON layer and might be incorrect for the measured part through the Si substrate due to different sputter yields for ITON and Si.

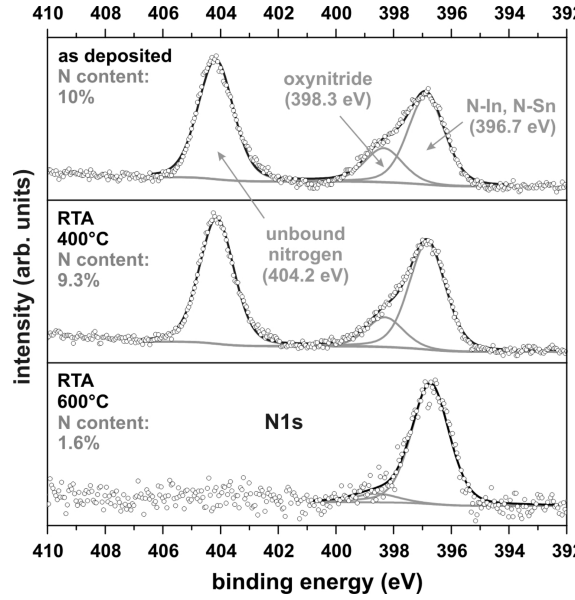

FIGURE 4. N1s core level spectra of ITON thin films after deposition and after RTA at 400 and 600 °C. Note that the scale of ordinates is varied for better visualization of the chemical states.

ITO films. These results are particularly important when ITON instead of ITO is applied where high annealing temperatures are required: e.g., for device processing with ITON as the TCO layer in InAlGaN-based optoelectronic devices.

The optical properties of the films were furthermore analyzed using a method based on analytical equations (12) which is capable of detecting and quantifying inhomogeneity effects. The extracted complex refractive index $n - ik$, where n is the refractive index and k is the extinction coefficient, revealed that, after annealing at high temperature, ITON is more transparent than ITO in the ultraviolet region. While the optical gap is practically the same for both types of films, the absorption of ITO is stronger ($k_{ITON}/k_{ITO} \cong 0.7$ at $\lambda = 300$ nm). An analysis in the near-infrared region (13) shows that the derived carrier relaxation time is increased with the decrease of wavelength for both the ITO and the ITON films. This is a typical behavior consistent with impurity-induced electron scattering. Furthermore, after annealing at 600 °C, the relaxation time of the ITO appears to be longer compared to that of ITON. The lower structural quality of ITON implied by the shorter relaxation time is likely to be associated with the release of nitrogen observed by XPS and QMS, as will be discussed in detail below.

Surface Properties. Rf sputtered ITO(N) films exhibit a polycrystalline structure with a typical grain size of around 50 nm (7). The examination of the film morphology by AFM revealed that the roughness of the ITON films (rms 7−8 nm at a scan size of 5 × 5 μm^2) was almost twice as large compared to that of the prepared ITO (rms 3−4 nm). However, no apparent change in surface morphology and roughness due to rapid thermal annealing was observed.

In order to characterize the elemental distribution through the films as well as the chemical surface composition, Auger electron depth profiles and X-ray photoelectron spectra have been recorded. Figure 3 shows a typical AES profile of an as-prepared 200 nm thick ITON film on Si. The depicted profile provides important qualitative information. Nevertheless, it is important to note that the plotted Auger intensities (which are not corrected for sensitivities toward the particular transition) do not directly reflect the quantitative elemental composition of the film. In addition, one has to keep in mind that the detected chemical composition might differ from the original atomic concentration due to preferential sputtering. In particular, an In enrichment due to this effect is observed for several In-containing compounds. Thus, the observed intensity increase of the In signal by about 5% within the first 60 min is very likely to be caused by preferential sputtering. Moreover, the different Auger transitions lead to different kinetic energies of the emitted electrons, which leads to a different probing depth. This effect may explain the slight difference of the interface position (half of the bulk intensity of the respective element) visible in Figure 1, since the Si signal provides a higher surface sensitivity compared to the ITON-related features. However, it can be noticed that the incorporated nitrogen is not homogeneously distributed throughout the ITON film but, rather, is accumulated within the upper quarter of the layer (∼40−50 nm). In deeper regions, the N signal decreases below the detection limit. On the other hand, a quite homogeneous distribution is found for indium, tin, and oxygen.

The incorporation of nitrogen into the ITON structure was examined in more detail by XPS measurements of the N1s core level. The results for films annealed at different temperatures are presented in Figure 4. Without any annealing of the samples three different nitrogen states exist in the material, having binding energies of 396.7, 398.3, and ∼404.2 eV, respectively.

The feature at 396.7 eV is attributed to nitrogen bound to metal atoms (N−In and N−Sn bonds). The binding energies of nitrogen atoms bound to these two species are almost the same (14, 15), and a separation between these

Downloaded by TECHNISCHE UNIV ILMENAU on July 29, 2009
Published on June 9, 2009 on http://pubs.acs.org | doi: 10.1021/am900138f

Downloaded by TECHNISCHE UNIV ILMENAU on July 29, 2009
Published on June 9, 2009 on http://pubs.acs.org | doi: 10.1021/am900138f

two contributions is therefore beyond the energy resolution of the measurement. The second feature at 398.3 eV is found to originate from oxynitride bonds (16), where oxygen as well as metal atoms are located in the surroundings of the nitrogen atom (InN_xO_y). Typical N−O bonds located at 400.0 eV were found only on as-loaded samples, prior to the ion bombardment procedure (not shown). They are caused by oxidation of the surface under ambient conditions and can be easily removed by gentle sputtering—which has been performed in order to remove surface adsorbates and to avoid changes in composition due to preferential sputtering. The peak at 404.2 eV may be caused by two possible sources: (a) NO_2 bonds or (b) unbound nitrogen incorporated into the crystal structure. Since the rf sputtering process is performed in nitrogen plasma and no additional structure is detected in the O1s signal, we assign the feature at 404.2 eV to incorporated unbound nitrogen that has been formed due to the harsh deposition conditions. It is believed that the unbound nitrogen is mostly located at interstitial sites, similar to reports on the nitridation of III−V semiconductor surfaces (17, 18).

For a quantification of the amount of inserted nitrogen in the near surface region, the core level spectra were fitted using Gauss−Lorentz functions, after removal of a Shirley-type background. Under the assumption of a homogeneous distribution of all detected elements through the depth probed by the XPS measurement (more than 90% of the XPS signal originates from the top 5−6 nm of the film), the elemental proportion of nitrogen was calculated. As seen in Figure 4, in addition to a small reduction of the total nitrogen concentration from 10% to 9.3%, no changes concerning the nitrogen states were observed after annealing at 400 °C. This aspect changes drastically after annealing at 600 °C. The state at 404.2 eV disappeared completely as well as almost the entire oxynitride component and parts of the metal−N signal, reducing the total N content to 1.6%. Finally, after RTA at 800 °C the amount of incorporated nitrogen is below the detection limit of XPS.

QMS measurements during heating under UHV conditions were performed to analyze the temperature-dependent desorption of molecules from the film in situ by measuring the gas composition in the chamber. At temperatures above 550 °C a strong release of molecular nitrogen was observed, while at the same time only minor desorption of N_2O was detected. Furthermore, no release of NO, NO_2, or O_2 was detected. This finding is in very good agreement with the RTA-induced changes in the N1s signal observed by XPS.

Additionally, more information about the films after their annealing can be extracted by evaluating the core level peak shape. The as-deposited and the 400 °C annealed ITON samples exhibit narrow symmetric core level peaks at binding energies (BE) of 444.7, 486.5, and 530.2 eV for $In3d_{5/2}$, $Sn3d_{5/2}$, and O1s, respectively (not shown). For ITON films that have been annealed at $T \geq 600$ °C, as well as for all ITO films, independent of sample treatment, all core level peaks are broadened and exhibit an asymmetric peak shape, as exemplified for the $In3d_{5/2}$ core level in Figure 5. Summarizing extensive studies on ITO(N) films prepared between 150 and 550 W rf power, the asymmetry of the core levels appears for samples that have a relatively high carrier concentration.

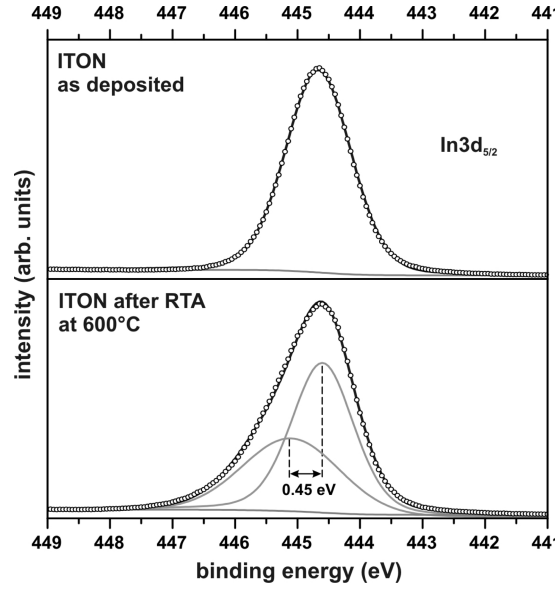

FIGURE 5. $In3d_{5/2}$ core level spectra of ITON thin films after deposition and after RTA at 600 °C.

According to previous reports (19, 20) this observation is explained by the response of the conduction electrons to the ionized atoms generated during the photoelectron emission process, which results in a splitting of the signal into a screened and an unscreened final state (19, 20). The peak shape of the unscreened contribution at higher binding energy is much broader compared to the screened one, since it involves excitation of plasmons. This intrinsic plasmon excitation is coupled with a certain relaxation rate, and as a result lifetime broadening of this contribution is expected, resulting in a Lorentzian peak profile. Hence, advancing the data analysis compared to the results in ref 21, where a fixed G/L ratio was assumed, resulting in a shift of 0.9 eV, and taking the different peak shapes for both components into account for fitting, the separation of the two components is only 0.45 eV, as shown in Figure 5. Note that the two different peaks, indicated in Figure 5, are not related to two different chemical In states but correspond to screened and unscreened final states. Following the model approach of ref 19, the energy separation corresponds to an estimated carrier concentration of 2×10^{20} cm^{-3}, which is in good agreement with the results from Hall measurements (see Figure 1). An analysis of the peak shape of ITON films annealed at various annealing temperatures leads to the conclusion that RTA at $T \geq 600$ °C results in an increase in the carrier concentration by about 1 order of magnitude, approaching the values for ITO that has been prepared in the same system using Ar as process gas. This effect is accompanied by segregation of Sn toward the surface, which has already been discussed in detail elsewhere for the ITON films (21).

The high electron concentration in indium−tin−oxide is caused by two factors: (a) the existence of a high content of

Downloaded by TECHNISCHE UNIV ILMENAU on July 29, 2009
Published on June 9, 2009 on http://pubs.acs.org | doi: 10.1021/am900138f

oxygen vacancies and (b) the incorporation of Sn atoms at In crystal sites leading to the effect of n-type doping (22). The amount of existing oxygen vacancies is mainly influenced by the deposition conditions during sputtering. Under reducing conditions, as in the case of the deposition of our ITO films in Ar plasma, the sputtering already results in the formation of a high concentration of oxygen vacancies and hence in a very high electron concentration for the films just after deposition. A totally different behavior is found when the material is sputtered from an ITO target using N_2 as discharge gas. In this case nitrogen is incorporated into the material. As described above, a large fraction of nitrogen is inserted unbound at interstitial sites while the other N atoms are incorporated in the surroundings of In, Sn, and O. It is anticipated that nitrogen decorates the sites where typically oxygen atoms are missing, resulting in trapping of electrons. This absence of oxygen vacancies leads to a much lower carrier concentration and hence a higher resistivity for these as-deposited ITON films. Since the incorporated nitrogen is not very strongly bound, it can be released by thermal treatments. Annealing above a critical temperature of ~550 °C causes desorption of nitrogen, which is completely removed after RTA at 800 °C. The remaining, previously N-decorated sites can now act as a source for electrons, resulting in a strong increase of the carrier concentration in the material. In this way, carrier concentration values comparable to those of Ar-sputtered ITO films are achieved. However, the lower mobility of the ITON films due to the removal of the incorporated nitrogen and In−N−O states resulted in ITON films with higher resistivity than the ITO films.

Contact Properties on p-Type GaN. For several samples the electrical contact behavior of ITON and ITO films was examined on p-type GaN layers by employing the c-TLM configuration and monitoring the current−voltage characteristics of the ring patterns with the shortest spacing (10 μm) with annealing temperature. For ~80% of the tested samples, stable $I-V$ characteristics could be obtained. Typical results are presented in Figure 6 (a) for the ITO film and (b) for the ITON film.

Obviously, as-prepared films did not show any ohmic behavior and, for annealing up to 800 °C, the ITO film never exhibited any linear ohmic characteristics. However, the ITON film forms an ohmic contact after annealing at 600 °C, but further annealing at higher temperatures deteriorated this characteristic, creating a nonohmic behavior. It is anticipated that the relatively high ohmic resistance of the ITON contact can be further reduced by optimizing the surface treatment of GaN. A procedure which is generally employed to form metal-based ohmic contacts on p-GaN is to use GaN layers with higher carrier concentration (in the range of 10^{18} cm^{-3}) than the ones used in this investigation. It has been reported that ITO can form an ohmic contact on p-GaN, with a carrier concentration in the range of 10^{17} cm^{-3}, only (a) after special surface treatment of the GaN surface (23), (b) by using a short period of superlattice tunneling contact layer (24), or (c) by inserting various thin

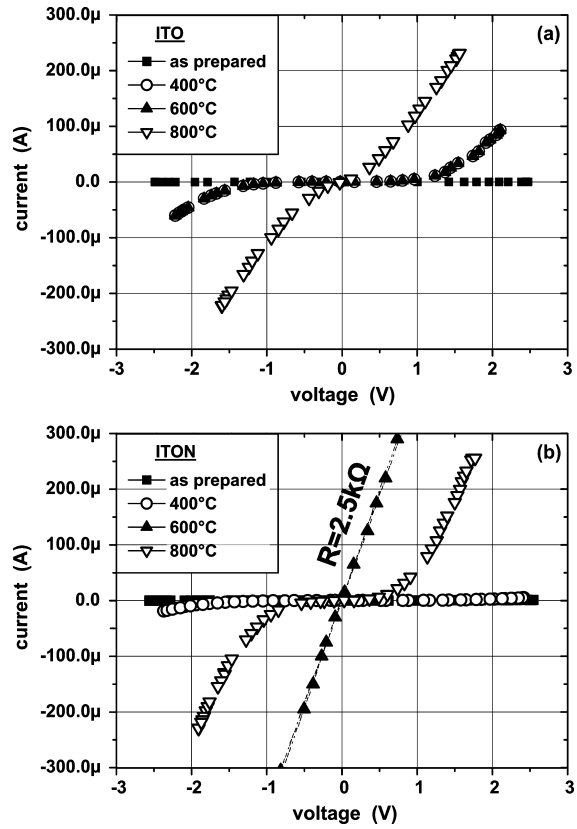

FIGURE 6. Current−voltage characteristics of (a) ITO and (b) ITON films as contacts on p-type GaN at different annealing temperatures.

metal layers between the GaN/ITO interface (25). It is important to note that the temperature of 600 °C, where the ITON film exhibited the ohmic behavior, is apparently related to the temperature of around 550 °C where the film showed the fastest release of incorporated nitrogen. However, the mechanism responsible for the realization of ohmic behavior of the ITON film on p-type GaN at the annealing temperature of 600 °C is not yet completely understood and further progress with respect to reproducibility is needed.

The mechanism might be associated with the diffusion of atoms through the ITON−GaN interface, creating an interfacial layer that changes the electronic properties at the interface. In this context it should be noted that a 100 nm thick rf sputtered ITON layer has been reported to form a Schottky contact on n-GaN based UV photodetectors after annealing at 600 °C for 15 min (6).

CONCLUSIONS

ITON and ITO films were fabricated by rf sputtering in nitrogen and argon plasma, respectively, and their properties were analyzed after high temperature annealing. The incorporated nitrogen in the ITON structure was found to form metal−N and oxynitride bonds or to exist in an unbound state. The distribution of the nitrogen within the as-deposited ITON films is not homogeneous. Most of the N is located in the upper 40−50 nm of the layer near the surface. The differences in ITO and ITON electrical properties are directly linked to the incorporated nitrogen which

decorates oxygen vacancies. However, it can be thermally removed to create a high degree of oxygen deficiency, thus resulting in a film with increased carrier concentration but high resistivity due to low mobility. The enhanced optical properties of the ITON films upon annealing were attributed to the incorporation of nitrogen into the structure. Ohmic contacts on p-type GaN could only be formed by ITON annealed at 600 °C. An optimized surface treatment of the GaN surface is believed to further improve the ohmic behavior of the ITON films, thus making ITON more preferable than ITO as a transparent and conductive material for GaN-based optoelectronic devices.

Acknowledgment. This work was supported by the research program IKYDA 03, partially by the EU project "GaNano", by the Thüringer Ministerium für Wirtschaft, Technologie und Arbeit (TMWTA) through the project INOZON (B509-04011), by the INTERREG IIIA Greece-Cyprus 2000-2006, and by the Research Grant Fraunhofer "Attract".

REFERENCES AND NOTES

(1) Margalith, T.; Buchinsky, O.; Cohen, D. A.; Abave, A. C.; Hansen, M.; DenBaars, S. P.; Coldren, L. A. *Appl. Phys. Lett.* **1999**, *74*, 3930.
(2) Su, S.-H.; Hou, C.-C.; Yokoyama, M.; Chen, S.-M. *J. Electrochem. Soc.* **2006**, *153*, G87.
(3) Shigesato, Y.; Paine, D. C.; Haynes, T. E. *J. Appl. Phys.* **1993**, *73*, 3805.
(4) Minami, T.; Kakumu, T.; Shimokawa, K.; Takata, S. *Thin Solid Films* **1998**, *317*, 318.
(5) Hultaker, A.; Jarrendahl, K.; Lu, J.; Granqvist, C.-G.; Niklasson, G. A. *Thin Solid Films* **2001**, *392*, 305.
(6) Zhang, B.; Dong, X.; Xu, X.; Zhao, P.; Wu, J. *Sol. Energy Mater. Sol. Cells* **2008**, *92*, 1224.
(7) Aperathitis, E.; Bender, M.; Cimalla, V.; Ecke, G.; Modreanu, M. *J. Appl. Phys.* **2003**, *94*, 1258.
(8) Aperathitis, E.; Modreanu, M.; Bender, M.; Cimalla, V.; Ecke, G.; Androulidaki, M.; Pelekanos, N. *Thin Solid Films* **2004**, *450*, 101.
(9) Koufaki, M.; Sifakis, M.; Iliopoulos, E.; Pelekanos, N.; Modreanu, M.; Cimalla, V.; Ecke, G.; Aperathitis, E. *Appl. Surf. Sci.* **2006**, *253*, 405.
(10) Krischok, S.; Yanev, V.; Balykov, O.; Himmerlich, M.; Schaefer, J. A.; Kosiba, R.; Ecke, G.; Cimalla, I.; Cimalla, V.; Ambacher, O.; Lu, H.; Schaff, W. J.; Eastman, L. F. *Surf. Sci.* **2004**, *566−568*, 849.
(11) Himmerlich, M.; Krischok, S.; Lebedev, V.; Ambacher, O.; Schaefer, J. A. *J. Cryst. Growth* **2007**, *306*, 6.
(12) Kondilis, A.; Modreanu, M.; Aperathitis, E. *Thin Solid Films* **2007**, *515*, 8586.
(13) Kondilis, A.; Aperathitis, E.; Modreanu, M. *Thin Solid Films* **2008**, *516*, 8073.
(14) Bu, Y.; Ma, L.; Lin, M. C. *J. Vac. Sci. Technol., A* **1993**, *11*, 2931.
(15) Inoue, Y.; Nomiya, M.; Takai, O. *Vacuum* **1998**, *51*, 673.
(16) Bello, I.; Lau, W. M.; Lawson, R. P. W.; Foo, K. K. *J. Vac. Sci. Technol., A* **1992**, *10*, 1642.
(17) Hecht, J.-D.; Frost, F.; Hirsch, D.; Neumann, H.; Schindler, A.; Preobrajenski, A. B.; Chasse, T. *J. Appl. Phys.* **2001**, *90*, 6066.
(18) Hecht, J.-D.; Frost, F.; Chasse, T.; Hirsch, D.; Neumann, H.; Schindler, A.; Bigl, F. *Appl. Surf. Sci.* **2001**, *179*, 196.
(19) Christou, V.; Etchells, M.; Renault, O.; Dobson, P. J.; Salata, O. V.; Beamson, G.; Egdell, R. G. *J. Appl. Phys.* **2000**, *88*, 5180.
(20) Egdell, R. G.; Walker, T. J.; Beamson, G. *J. Electron Spectrosc. Relat. Phenom.* **2003**, *128*, 59.
(21) Himmerlich, M.; Koufaki, M.; Mauder, Ch.; Ecke, G.; Cimalla, V.; Schaefer, J. A.; Aperathitis, E.; Krischok, S. *Surf. Sci.* **2007**, *601*, 4082.
(22) Gonzalez, G. B.; Mason, T. O.; Quintana, J. P.; Warschkow, O.; Ellis, D. E.; Hwang, J.-H.; Hodges, J. P.; Jorgensen, J. D. *J. Appl. Phys.* **2004**, *96*, 3912.
(23) Kim, D. W.; Sung, Y. J.; Park, J. W.; Yeom, G. Y. *Thin Solid Films* **2001**, *398−399*, 87.
(24) Chang, C. S.; Chang, S. J.; Su, Y. K.; Lai, W. C.; Kuo, C.-H.; Wang, C. K.; Lin, Y. C.; Hsu, Y. P.; Skei, S. C.; Lo, H. M.; Ke, J. C.; Sheu, J. K. *Phys. Status Solidi C* **2003**, *0*, 2227.
(25) Chae, S. W.; Kim, K. C.; Kim, D. H.; Kim, T. G.; Yoon, S. K.; Oh, B. W.; Kim, D. S.; Kim, H. K.; Sung, Y. M. *Appl. Phys. Lett.* **2007**, *90*, 181101.

AM900138F

Downloaded by TECHNISCHE UNIV ILMENAU on July 29, 2009
Published on June 9, 2009 on http://pubs.acs.org | doi: 10.1021/am900138f